CURVE CROSSING FOR LOW ENERGY ELASTIC SCATTERING OF He^+ BY Ne*

by

S. M. Bobbio†
L. D. Doverspike
R. L. Champion

Department of Physics
College of William and Mary
Williamsburg, Virginia 23185

*Work supported in part by the National Science Foundation and by NASA Grant No. NGL-47-006-055

†Present Address: Department of Chemistry, Brown University, Providence, Rhode Island.

Abstract

The perturbation seen in the experimental differential elastic scattering cross section for the 40eV He^+ + Ne system has been attributed to a single crossing of two intermolecular potential energy curves. A new theoretical treatment of the curve crossing problem, namely that of Delos and Thorson, is employed to obtain the crossing probabilities and phases associated with the crossing. These are determined by utilizing *ab initio* potentials involved in the crossing and are further used in a partial wave calculation of the cross section, which is compared with our experiment. The origin of the oscillatory structure observed in the differential cross section is discussed in semi-classical terms by defining the problem in terms of two pseudo-deflection functions. A rainbow effect is shown to be related to a particular feature (a maximum rather than a minimum) of these deflection functions.

I. Introduction

Extensive studies of the differential scattering of singly charged rare gas ions by rare gas atoms have been reported by several laboratories[1]. These efforts have contributed greatly to our theoretical understanding of elastic scattering and various inelastic processes which generally involve several potentials and interactions of the electronic states of the collision partners. The more detailed theoretical analysis which is needed to cope with such problems is currently in a state of rapid development. For example, a unified formal treatment of the two-state potential curve crossing problem for atomic collisions has just been completed by Delos and Thorson[2]; this treatment of the two-state problem being more complete than the standard Landau-Zener-Stuckleberg method which has been used in many calculations heretofore. Briefly, the approach developed by Delos and Thorson essentially reduces the problem of solving the two coupled second order wave equations to the easier task of solving three first order "trajectory equations". Their solutions are readily connected with the S-matrix elements describing the scattering amplitudes for the two state system. The inputs to such a calculation are the potential curves in question (either a diabatic or adiabatic representation will suffice) and the interaction term $V_{12}(R)$ in the vicinity of the crossing.

The purposes of this paper are to: 1) demonstrate the results of such a calculation for the scattering system He^++Ne (E_{cm}=40eV), where the initial inputs are from an <u>ab initio</u> calculation of Sidis and Lefebvre-Brion[3] for the $NeHe^+$ molecular ion; 2) compare these results with the differential elastic scattering cross section measured in this laboratory; 3) suggest a

slight modification in the potentials (which probably isn't unique) which is necessary to bring certain features of the calculation and experiment into fairly good agreement and; 4) disucss the origin of the observed scattering features in semiclassical terms.

II. A Summary of the Theory

The recent theoretical work of Delos and Thorson[2], (to which the reader should refer for complete details of the theory) has reduced the two coupled Schroedinger equations which are assumed to govern the dynamics of the scattering, to the three first order equations:

$$\frac{dZ(\ell,t)}{dt} = -\frac{\sqrt{1-Z^2(\ell,t)}}{2(1+t^2)}\cos[\Delta+\Gamma_2(\ell,t)-\Gamma_1(\ell,t)]$$

$$\frac{dZ}{dt}(\ell,t) = \frac{Z(\ell,t)}{2(1+t^2)\sqrt{1-Z^2(\ell,t)}}\sin[\Delta+\Gamma_2(\ell,t)-\Gamma_1(\ell,t)] \qquad (1)$$

$$\frac{d\Gamma_2(\ell,t)}{dt} = \frac{\sqrt{1-Z^2(\ell,t)}}{2(1+t^2)\,Z(\ell,t)}\sin[\Delta+\Gamma_2(\ell,t)-\Gamma_1(\ell,t)]$$

with

$$\Delta = -\frac{\beta}{2}\int_{-\epsilon}^{t}\frac{\sqrt{1+\tau^2}}{\sqrt{\epsilon+\tau}}\,d\tau$$

and the boundary conditions

$$Z(\ell,-\epsilon) = 0$$
$$\Gamma_1(\ell,-\epsilon) = 0$$
$$\Gamma_2(\ell,-\epsilon) = -\pi$$

The quantities β and ϵ depend upon the angular momentum quantum number, ℓ, and the potential parameters through the relations:

$$\epsilon = \frac{1}{2}\left[E - V_1(R_c) - \frac{\hbar^2(\ell+\frac{1}{2})^2}{2\mu R_c^2}\right] \cdot \frac{\left(\left.\frac{dV_1}{dR}\right|_{R_c} - \left.\frac{dV_2}{dR}\right|_{R_c}\right)}{V_{12} \cdot F(R_c)} \quad ,$$

$$\beta = \frac{4}{\hbar}\left\{\frac{\mu V_{12}^3(R_c)}{\left(\left.\frac{dV_1}{dR}\right|_{R_c} - \left.\frac{dV_2}{dR}\right|_{R_c}\right) F(R_c)}\right\}^{1/2}$$

where $V_{12}(R_c)$ is the interaction term, V_1 and V_2 are the two potential curves as defined in Fig. 1; $F(R_c)$ is the geometric average of $\left[dV_{1eff}/dR\right]_{R_c}$ and $\left[dV_{2eff}/dR\right]_{R_c}$ and the subscript c refers to the crossing.

The set of equations (1) are numerically integrated for each value of ℓ from $t = -\epsilon$ to $t = +\infty$ (in practice the quantities $\Gamma_1(\ell,t)$, $\Gamma_2(\ell,t)$, and $Z(\ell,t)$ have attained their asymptotic values for $t = +30$ at which point the integration is halted). The solutions $\Gamma_1(\ell)$, $\Gamma_2(\ell)$, and $Z(\ell)$ have the same general validity in the semiquantal regime as do the JWKBL phase shifts, even in the important case where the classical turning point is close to the crossing. Moreover, these solutions are connected with the elastic scattering problem in the following way:

$$f(\theta) = \frac{1}{2ik}\sum_{\ell=0}^{\infty}(2\ell+1)P_\ell(\cos\theta)\left[S(\ell)-1\right] \quad , \qquad (2)$$

$$S(\ell) = Z^2(\ell)\exp\left[2i\left[\eta_a(\ell) - \Gamma_2(\ell)\right]\right] +$$

$$\left[1-Z^2(\ell)\right]\exp\left[2i\left[\eta_a(\ell) + \Gamma_1(\ell)\right]\right] .$$

Here, $\eta_a(\ell)$ is the JWKBL phase shift resulting from scattering by the ground state adiabatic potential (i.e., $V_a(R)$ in Fig. 1).

For a small interaction term, $V_{12}(R_c)$, it is necessary to solve the set (1) only over a relatively narrow range of ℓ around ℓ_c. Outside this range the Landau-Zener transition probability is a very good approximation to $Z^2(\ell)$; $\Gamma_1(\ell)$ is constant, approximately $\pi/4$; and $\Gamma_2(\ell)+\pi$ is essentially the difference between $\eta_a(\ell)$ and $\eta_d(\ell)$, where the latter quantity is the phase shift corresponding to the diabatic potential (i.e., $V_1(R)$ in Fig. 1) which connects to the ground state of the separated atom and ion.

III. Analysis of the Scattering Data

In Fig. 2 are shown the experimental elastic differential cross sections for the He^++Ne system at three different energies. At 6eV the cross section is smooth and monotonically decreasing. At 30eV a perturbation in the differential cross section appears at large angles. At 40eV the major portion of this perturbation is centered in the angular range of our apparatus (for a description of the apparatus, see ref. 4), and it is to this data that the present analysis will be directed. It will be assumed in the subsequent analysis that these perturbations are due to a single crossing of the $B^2\Sigma^+$ and $C^2\Sigma^+$ states of $NeHe^+$.

An analytic function for the adiabatic curve was carefully constructed using the ab initio calculated points of Sidis[3] as shown in Fig. 3; the small value which he obtained for the interaction term ($V_{12}(R_c)$=.26eV) necessitated a sharp "knee" in the adiabatic potential. The functions $Z(\ell)$, $\Gamma_1(\ell)$, and $\Gamma_2(\ell)$ were found by numerical integration of the set (1), and the partial wave sum utilizing eqns. (2) was carried to 1600 terms to evaluate the cross section.

The result showed that the predicted perturbation was located at too small an angle (about a 7° shift to the left relative to the experimental data). Putting aside uniqueness considerations, the crossing point was shifted up by 1.3 eV as shown by the solid lines in Fig. 3. Using these two new curves and the parameters

$$\left.\frac{dV_1}{dR}\right|_{R_c} - \left.\frac{dV_2}{dR}\right|_{R_c} = 35.0 \text{ eV}/a_o$$

$$V_{12}(R_c) = 0.26 \text{ eV}$$

$$R_c = 1.86\ a_o$$

$$F(R_c, \ell_c) = 35.74 \text{ eV}/a_o$$

the calculation was again performed with the result shown in Fig. 4. The perturbations in the theoretical prediction are seen to be in quantitative agreement with those resolved in the experiment. Furthermore, the qualitative aspects of the experimental cross section (a smooth decrease before and fairly smooth, with minor oscillations, after the crossing perturbation) are satisfactorily reflected by the calculation. The major difference between the relative differential cross section $c\cdot\sigma_{expt}(\theta)$, and $\sigma_{calc}(\theta)$ is in the general decay rate of the cross section.

In determining $c\cdot\sigma_{expt}(\theta)$ from the observed laboratory scattering intensity, the latter was first corrected for thermal and kinematic effects which have been discussed by Lorents and Conklin[5]. This was done by measuring (at 5 degree intervals) the energy distribution function for the

elastic channel and fitting the observed FWHM to a form

$$FWHM(\theta) = 1 + a\cdot\theta,$$

and the laboratory intensities were corrected accordingly. Subsequently the normal "scattering volume" correction was made and the appropriate Jacobian employed to retrieve $c\cdot\sigma_{expt}(\theta)$.

If one chose to equate the two functions, $c\cdot\sigma_{expt}(\theta)$ and $\sigma_{calc}(\theta)$, at an angle $20^{\circ}<\theta<30^{\circ}$, then a rather noticable disagreement is the two functions would be observed for large scattering angles. Assuming that a normalization of $c\cdot\sigma_{expt}(\theta)$ at $\theta = 25^{\circ}$ to $\sigma_{calc}(25^{\circ})$ is reasonable, one might ask: what <u>systematic</u> experimental error (as a function of θ) could occur for $\theta > 25^{\circ}$? The horizontal lines in Fig. 4 indicate a conservation estimate ($\pm 0.4\sigma_{expt}(75^{\circ})$) of such a systematic error. Based on this normalization scheme, it is clear that there exists a significant difference in $\sigma_{calc}(\theta)$ and $\sigma_{expt}(\theta)$ for post perturbation angles. Two possible explanations for this disagreement are readily apparant: 1) the <u>ab initio</u> diabatic potential ($V_1(R)$) utilized in the calculation is too "hard" for $R<R_c$; or 2) the two state approximation is not sufficient, i.e., the elastic channel may be depleted for $\theta > 50^{\circ}$ by other nearby crossings. Since no measurements of the inelastic differential cross sections were made, no attempt to distinguish between these two possibilities has been made.

IV. Semiclassical Interpretation

In order to discuss the origin of the observed scattering features in semiclassical terms, two pseudo-deflection functions $\Theta_1(\ell)$ and $\Theta_2(\ell)$ have been defined:

$$\Theta_1(\ell) = 2\frac{d}{d\ell}\left[\eta_a(\ell) + \Gamma_1(\ell)\right]$$

$$\Theta_2(\ell) = 2\frac{d}{d\ell}\left[\eta_a(\ell) - \Gamma_2(\ell)\right]$$

These functions have been constructed by extending the equivalence relation to the arguments which appear in the partial wave sum in equation (2).

$\Theta_1(\ell)$ and $\Theta_2(\ell)$ have been plotted along with the adiabatic and diabatic deflection functions $\Theta_a(\ell)$ and $\Theta_d(\ell)$ in Fig. 5. $\Gamma_1(\ell)$ is essentially a step function around ℓ_c (the angular momentum for which the classical turning point equals R_c); this produces a negative pulse in the deflection function ($\Theta_1(\ell)$) which serves to decrease $\Theta_a(\ell)$ only in the region immediately to the left of ℓ_c. As previously mentioned when ℓ becomes small

$$\Gamma_2(\ell) \longrightarrow \eta_a(\ell) - \eta_d(\ell) - \pi$$

so that to the left of ℓ_c

$$\Theta_2(\ell) \longrightarrow \Theta_d(\ell)$$

The difference between $\Theta_2(\ell)$ and $\Theta_d(\ell)$ is the approximately wedge-shaped region of area 2π which has been removed from $\Theta_d(\ell)$ around ℓ_c.

In our numerical procedures we have not solved the set (1) over the entire range of ℓ. For $\ell - \ell_c \gtrsim 16$, $Z(\ell)$ is almost zero and $Z^2(\ell)$ is entirely negligible. Consequently, for large ℓ, the adiabatic phase shifts are all that need be calculated. Similarly, for ℓ in the region $\ell_c - \ell \gtrsim 20$, $\Theta_2(\ell)$ has converged to $\Theta_d(\ell)$. In this same region $\Gamma_1(\ell)$ has been extrapolated; this makes negligible difference in the resulting calculation since

$\Gamma_1(\ell)$ has attained its limit (approximately $\pi/4$) and makes no further contribution to $\Theta_1(\ell)$. In this region the Landau-Zener approximation has been used for $Z^2(\ell)$, that is:

$$Z^2(\ell) = \exp\left\{-2\pi\hbar^2\left[\left(\left.\frac{dV_1}{dR}\right|_{R_c} - \left.\frac{dV_2}{dR}\right|_{R_c}\right)v(R_c,\ell)\right]^{-1}\cdot V_{12}^2(R_c)\right\}$$

The semiclassical predictions of $\Theta_1(\ell)$ and $\Theta_2(\ell)$ for the differential cross section may now be stated; here, references to angles and values of ℓ will be to Fig. 5. For $\theta > \theta_3$ there are two paths the system may follow, i.e. $\Theta_1(\ell) = \Theta_a(\ell)$ and $\Theta_2(\ell) = \Theta_d(\ell)$. Since $Z(\ell)$ is almost unity $\Theta_d(\ell)$ basically accounts for the differential cross section in this region. Since $Z(\ell)$ is not identically unity however, there should be some small amplitude oscillations in $\sigma(\theta)$ for $\theta > \theta_3$. A straight forward semiclassical treatment shows that the cross section should oscillate with periodicity

$$\Delta\theta = \frac{2\pi}{\Delta\ell} \qquad (3)$$

and amplitude of approximately one tenth the average intensity. Furthermore, equation (3) is found to be valid for all angles larger than θ_o i.e., equation (3) predicts the periodicities of the high frequncy oscillations of the calculated differential cross sections in this angular region. Since only one classical trajectory $\Theta_1(\ell) = \Theta_a(\ell)$ exists for $\theta < \theta_o$ all oscillations are damped out in this region.

Olson and Smith[19] have pointed out that the minimum in Θ_a could give rise to a rainbow effect in the differential cross section. However, by referring to the graph of $Z^2(\ell)$ it is apparant that the probability that the system will undergo a deflection of θ_o is very small. Consequently this rainbow effect should not appear in differential cross section. If the coupling were stronger, the effects of this broad minimum would probably be quite spectacular.

The large "rainbow-like" envelope (at 52^o) in the cross section is essentially due to the negatively curved double-valued portion of $\Theta_1(\ell)$ immediately to the right of ℓ_c. Since $\Theta_1(\ell)$ possesses the other double-valued portion to the left of ℓ_c, this last assertion should be verified. In order to do so a large negative pulse has been added to $\Theta_1(\ell)$ in the vicinity of its minimum and the cross section recalculated. The results are shown in Fig. 6. Since the rainbow structure has only moved about 2^o, the small amount by which the maximum of $\Theta_1(\ell)$ has changed instead of the large change effected at its minimum, the initial assertion is believed to be correct. Also, since the multiplicity of (the distorted) $\Theta_1(\ell)$ has been extended to include angles less than θ_o, the higher frequency oscillations appear at smaller angles.

V. Conclusion

Intermolecular potentials very similar to the ab initio potentials of Sidis along with the semiquantal method of Delos and Thorson have been utilized in a calculation of the elastic differential cross section and compared to the experimental results. In this particular problem ($He^+ + Ne$)

the region in which the "trajectory equations" must be solved to obtain the transition probability and the corresponding phase shifts extends over a small range of angular momenta, so that the numerical work is not too formidable and the correct evaluation of these quantities is seen to provide better agreement with experiment (particularly in the elastic scattering in the region most sensitive to the crossing) than did earlier treatments of this problem. Furthermore, the Delos-Thorson treatment lends itself to a semi-classical interpretation, which is shown to be capabel of shedding considerable light on the basic physics associated with the two-state crossing problem.

Acknowledgements

We would like to thank J. Delos for many valuable discussions related to his work and to W. G. Rich for his assistance in obtaining the experimental data.

References

1. See for example:
   a) F. T. Smith, R. P. Marchi, W. Aberth and D. C. Lorents, Phys. Rev. A161, 31 (1967).
   b) D. Coffey, Jr., D. C. Lorents and F. T. Smith, Phys. Rev. A187, 201 (1969).
   c) F. T. Smith, H. H. Fleischmann and R. A. Young, Phys. Rev. A2, 379 (1970).
   d) R. L. Champion and L. D. Doverspike, J. Phys. B2, 1353 (1969).
   e) J. Baudon, M. Barat and M. Abignoli, J. Phys. B1, 1083 (1968).
   f) J. Baudon, M. Barat and M. Abignoli, J. Phys. B3, 207 (1970).
   g) R. E. Olson and F. T. Smith, Phys. Rev. A3, 1607 (1971).
2. J. B. Delos and W. R. Thorson, Phys. Rev. Letters 28, 647 (1972), and Phys. Rev. A XXX, (1972).
3. V. Sidis and H. Lefebvre-Brion, J. Phys. B: Atom. Molec. Phys. 4, 1040 (1971) and V. Sidis, Ph.D. dissertation, University of Paris (1971). The numerical values for the various potentials are only contained in the latter document.
4. R. L. Champion, L. D. Doverspike, W. G. Rich, S. M. Bobbio, Phys. Rev. A2, 2327 (1970).
5. D. C. Lorents and G. M. Conklin, to be published, Phys. Rev.

Figure Captions

Figure 1 Schematic diagram of the potential curves for $NeHe^+$ discussed in this paper. $V_1(R)$ and $V_2(R)$ are the results of diabatic calculations and $V_A(R)$ is an assumed adiabatic interaction.

Figure 2 Experimental differential elastic scattering cross sections for He^+ + Ne at; (a) 40eV, (b) 30eV, (c) 6eV.

Figure 3 Circles - result of the Sidis calculation, solid lines - analytic functions representing the adiabatic and diabatic curves corresponding to these circles, dashed line - curves which were used to calculate the differential cross section in figure 4.

Figure 4 Differential elastic scattering cross section, 40eV He^+ + Ne: solid line - calculation; points - experiment.

Figure 5 Inset - the function $Z^2(\ell)$; solid line - adiabatic deflection function Θ_a, chain line - diabatic deflection function Θ_d, dashed line - the pseudo deflection function Θ_2, dotted line - the pseudo deflection function Θ_1.

Figure 61 (Bottom) solid lines - $\Theta_1(\ell)$ and $\Theta_2(\ell)$ from figure 5, dashed line - the distortion introduced into Θ_1; (top) solid line - convoluted differential cross section corresponding to undistorted Θ_1 and Θ_2, dashed line - convoluted differential cross section where Θ_1 has been distorted. Both cross sections have been calculated for the 40eV He^+ + Ne elastic scattering system.

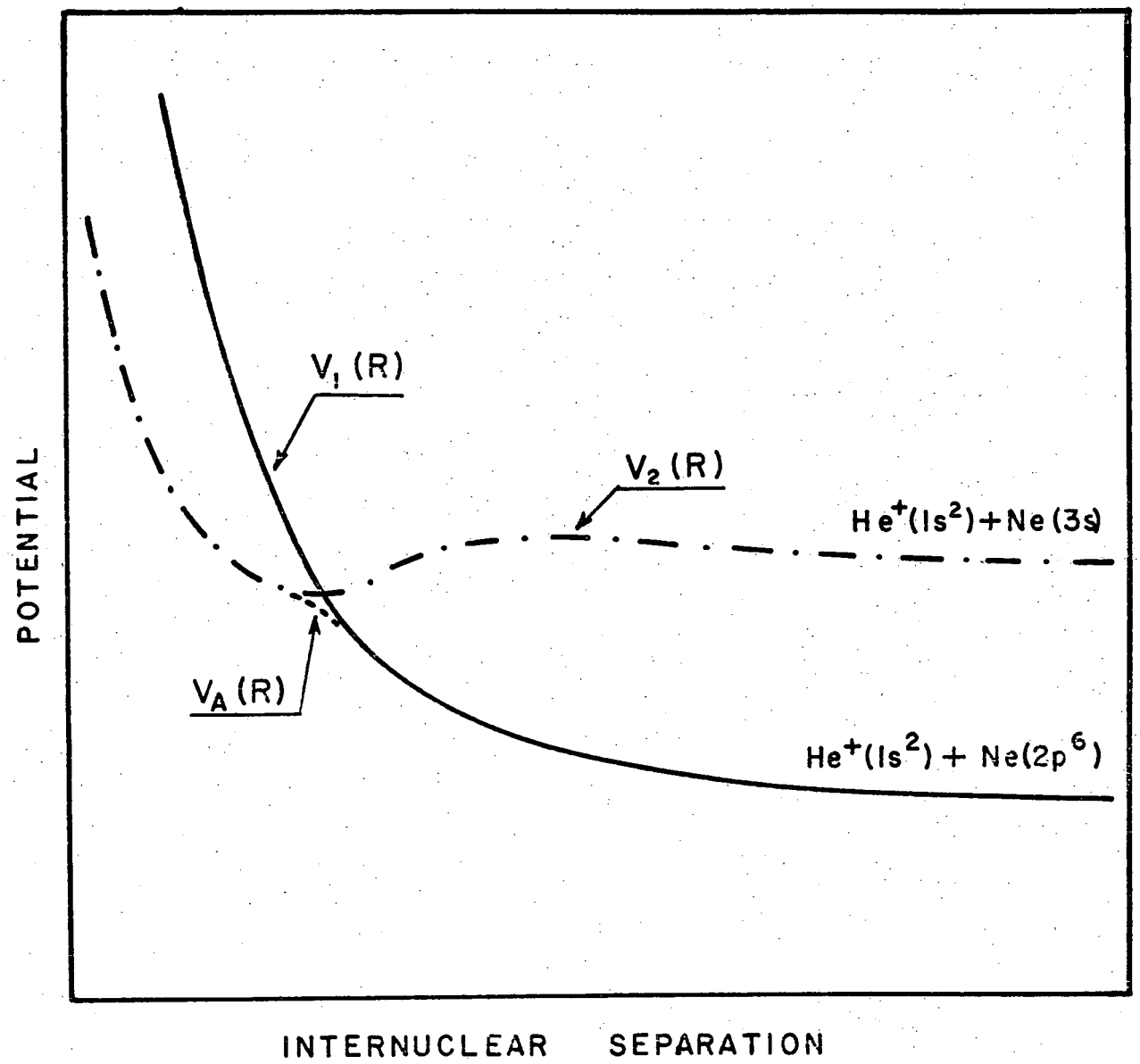

FIG. 1 Bobbio et al.

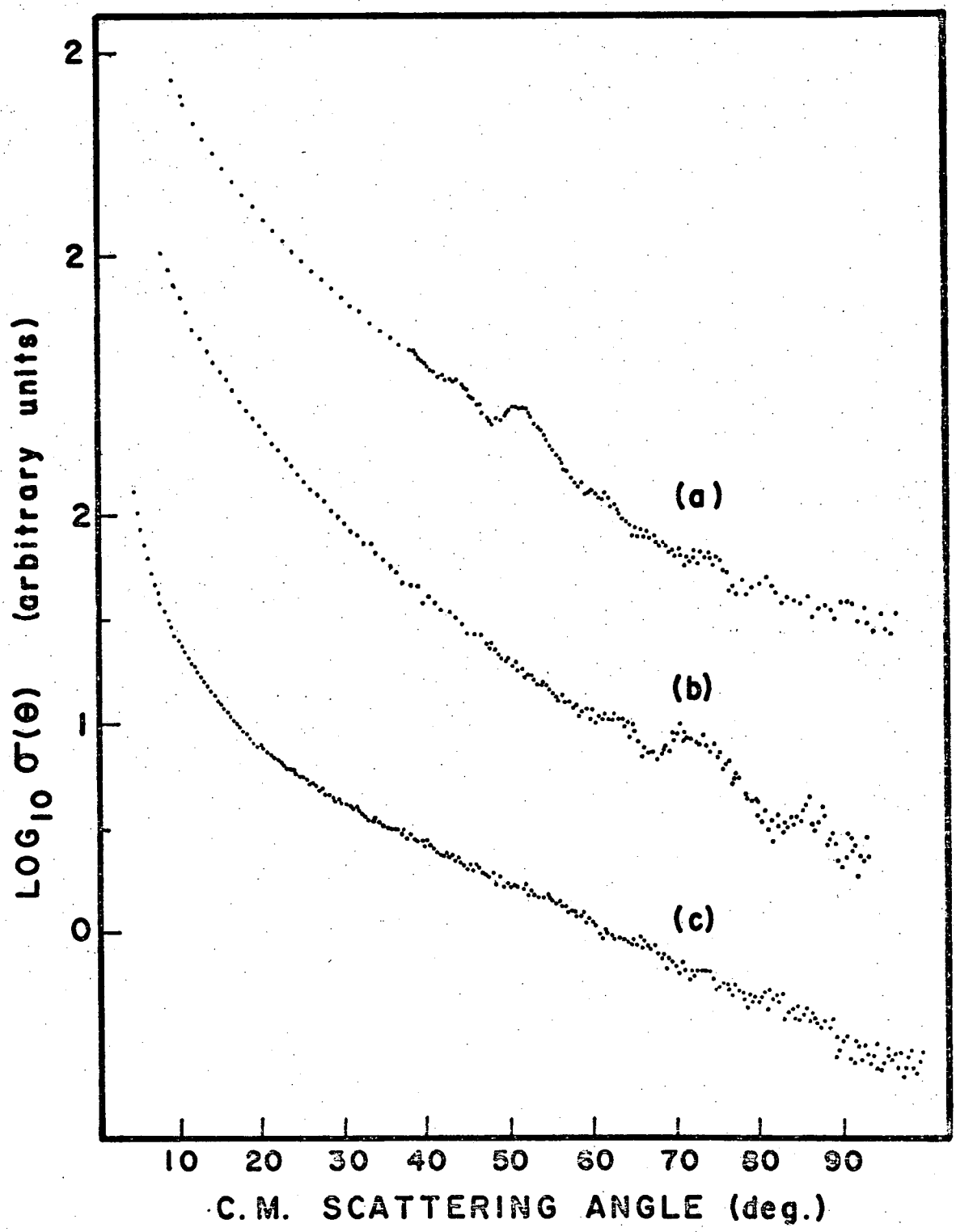

FIG. 2 BOBBIO et al.

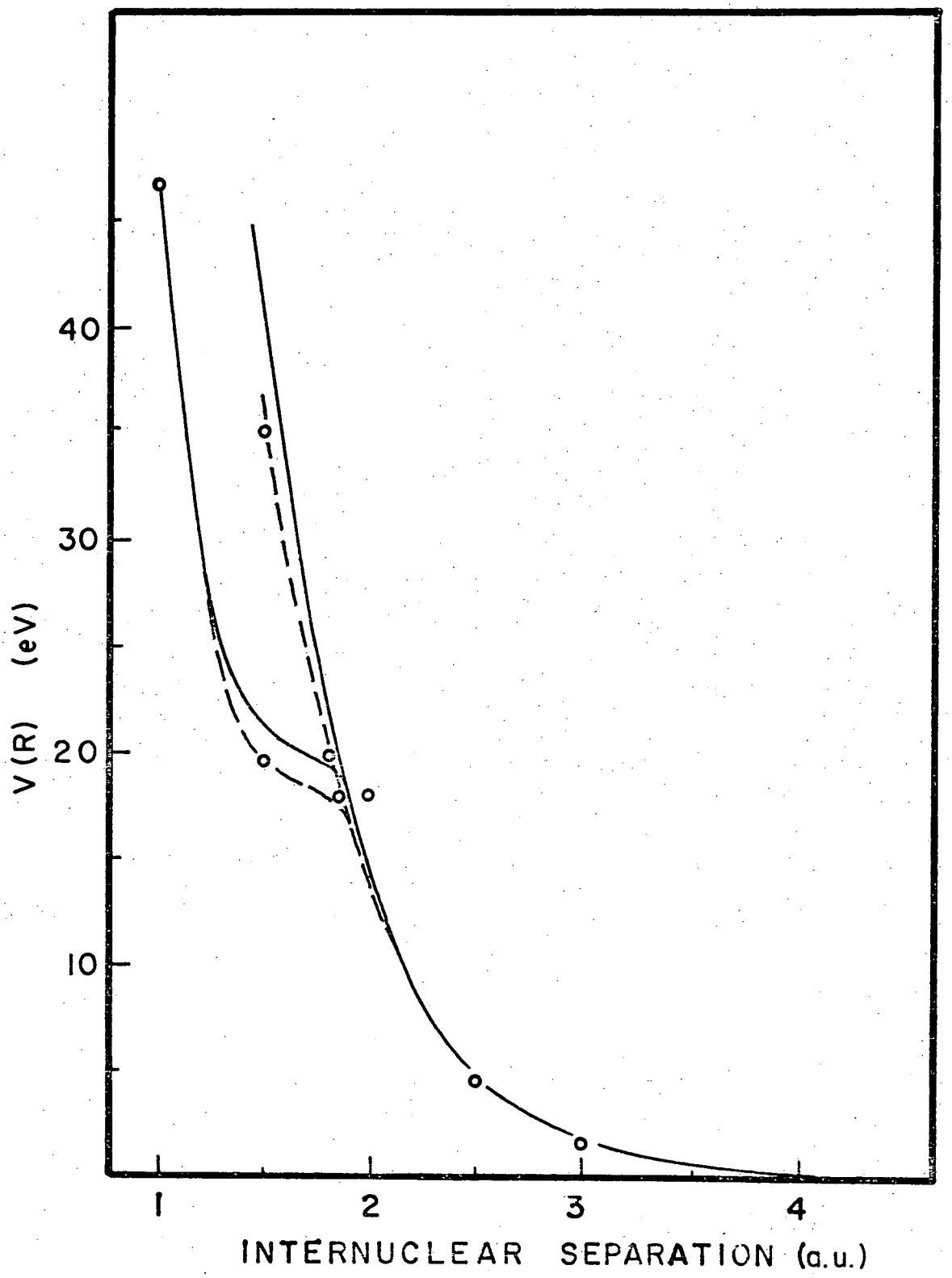

Fig 3 Bobbio et al.

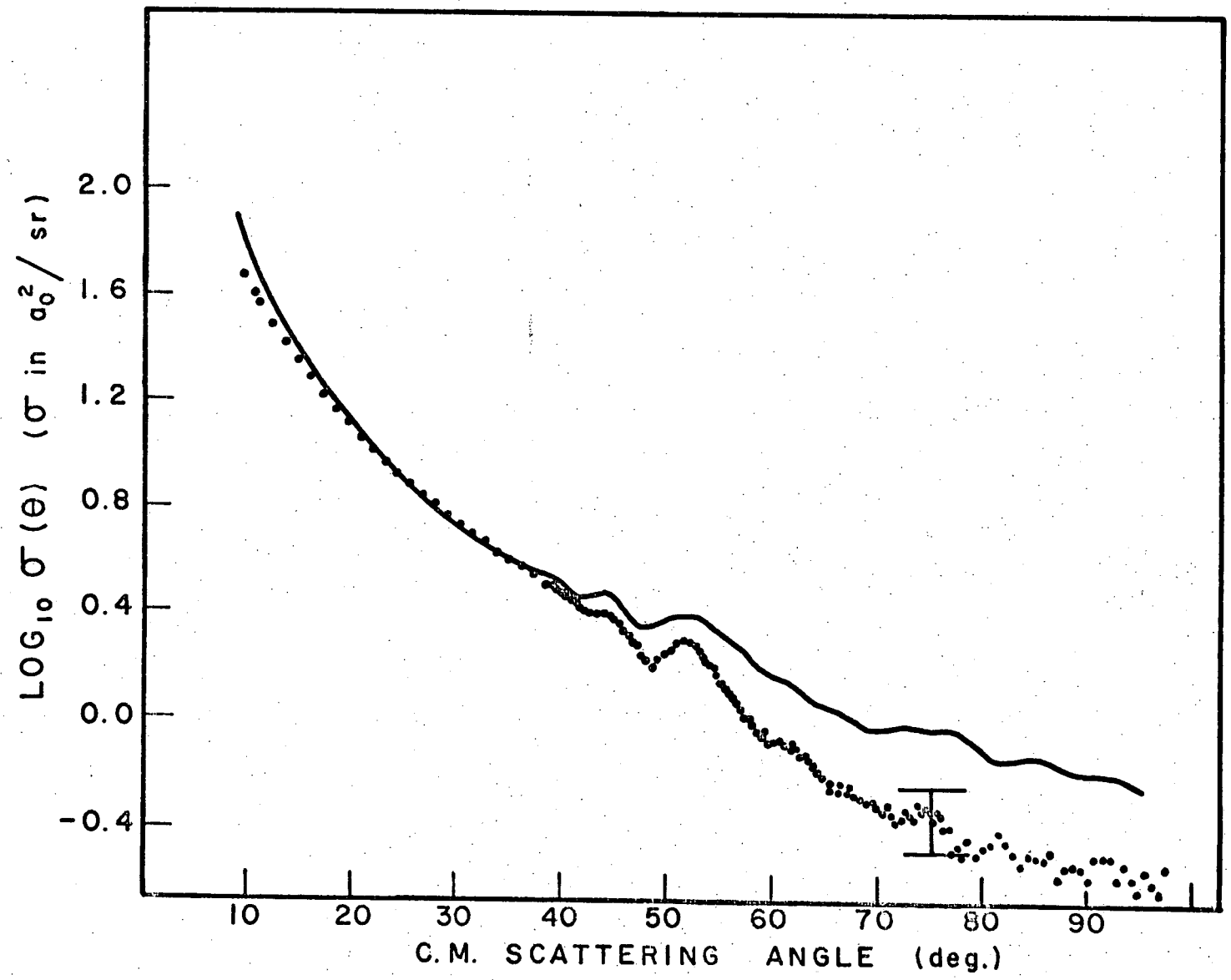

Rebbio et al. Fig 4

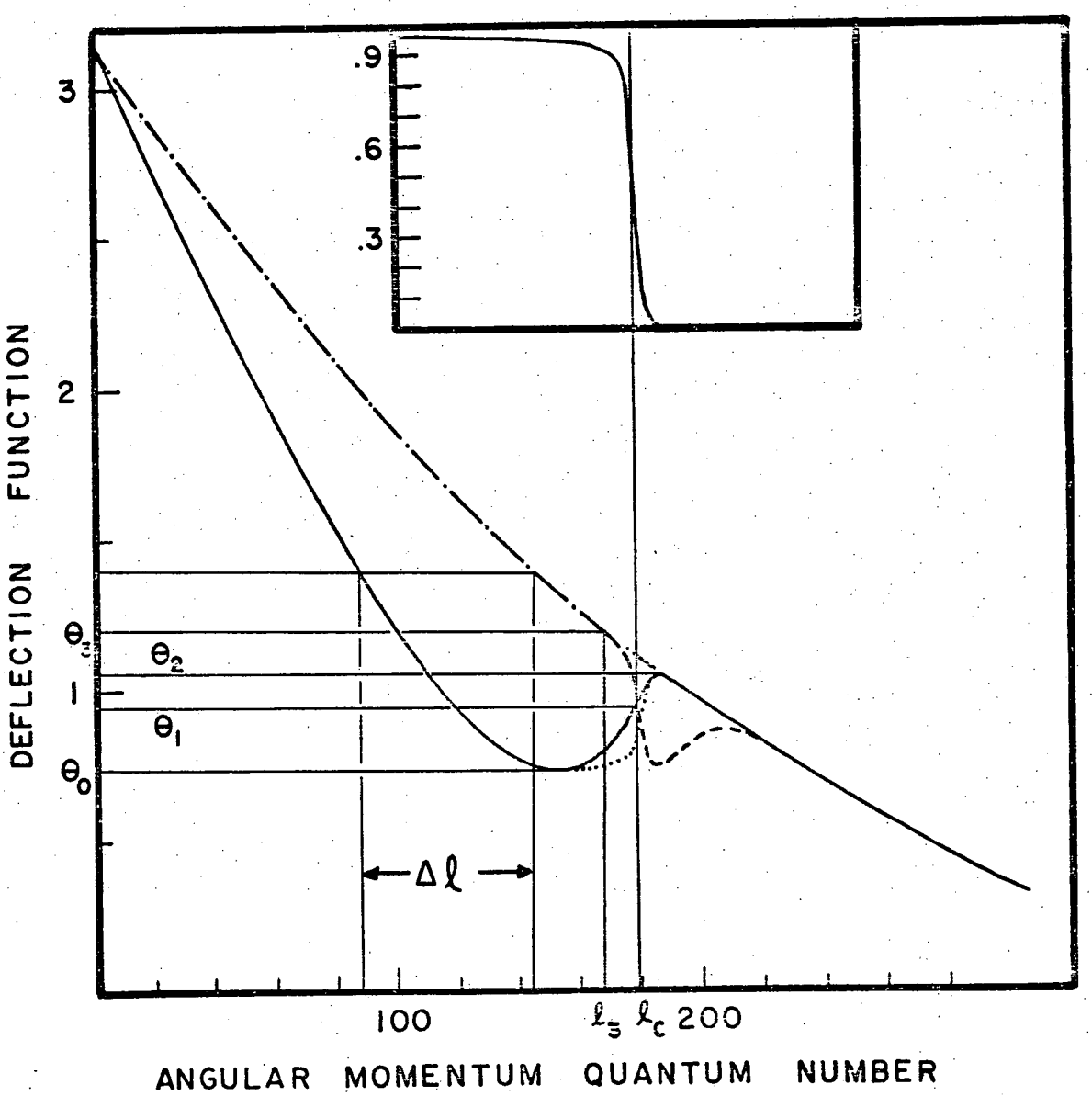

FIG 5. Bobbio et al.

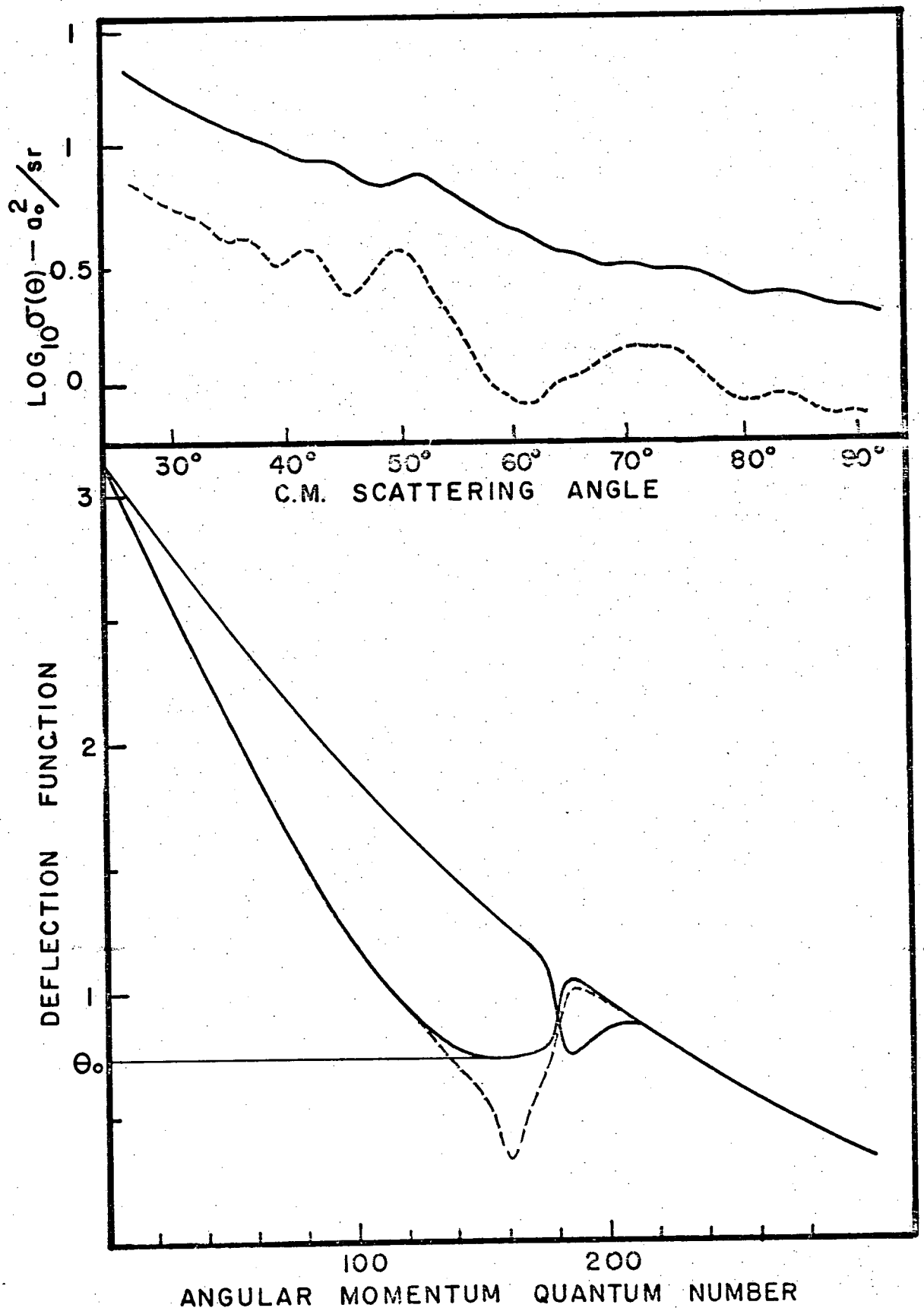

FIG 6 Bobbio et al